Structure-borne sound in buildings: Advances in measurement and prediction methods.

Barry Marshall Gibbs[a)] and Michel Villot[b)]

a) Acoustics Research Unit, School of Architecture, University of Liverpool, U.K.
    Email: bmg@liverpool.ac.uk
b) Consultant MV expert, 5 bis chemin Thiers, 38100 Grenoble, France
    Email: michel.jean.villot@gmail.com

This paper coincides with recent publications of international Standards, which provide methods of predicting the performance of both heavyweight and lightweight buildings in terms of airborne sound insulation and impact sound isolation, from the performance of individual elements such as walls and floors. The performances of the elements are characterized by the sound reduction index and the impact sound pressure level. To predict the sound pressure level due to vibrating sources (i.e. mechanical installations, water services and other appliances), source data is required in a form appropriate as input for prediction models similar to the above, i.e. as equivalent single quantities and frequency band-averaged values. Three quantities are required for estimating the structure-borne power for a wide range of installation conditions: activity (the free velocity or the blocked force of the operating source), source mobility (or the inverse, impedance) and receiver mobility (or impedance) of the connected building element. Methods are described for obtaining these source quantities, including by using laboratory reception plates. The paper concludes with a proposed database, based on laboratory measurements and simple mobility calculations, which provides a practical approach to predicting structure-borne sound in buildings.

1   INTRODUCTION

Structure-borne sound in buildings is generated by vibrating or impacting sources, which inject vibrations through the contacts with building elements. The vibrations propagate throughout the building and eventually radiate sound into adjacent spaces or non-adjacent spaces in the building. To predict structure-borne sound, a sub-structuring approach is required for both the passive[1, 2] (e.g. walls and floors involved in the sound transmission) and active components (e.g. plant equipment and water services, acting as the sound sources). Procedures are in place for the passive components in international Standards[3, 4]. The sound reduction indices and impact sound pressure levels of the building elements of interest are measured in Standard test facilities[5]. The measured data is modified, to include edge effects and dissipative losses, then incorporated into the building sound propagation models for prediction of in-situ performance. The prediction models also require input data for junctions between building elements, measured in Standard test facilities[6].

For the active components, the source quantities also require laboratory measurements, to provide input data for the building propagation models. For airborne sources, there is a menu of Standards for measuring the sound power levels[7], incorporated into a present Standard[8]. This Standard also deals with structure-borne sound source prediction using input data in the form of

installed power (power transmitted to the receiving building element to which the source is connected) but is only applicable to heavyweight buildings and is rather difficult to use. This Standard is now under review, to simplify the method for heavyweight buildings and to deal with lightweight buildings.

There is not yet a comprehensive menu of methods and data for structure-borne sound sources, but there has been recent progress on both source characterization[9], providing input data for prediction in any type of buildings, and prediction of in-situ performance[10] and a description of advances in this area forms the core of this paper. The paper concentrates on lightweight buildings, since the most recent developments have been on building elements, such as framed/ribbed cavity walls and floors. Note that some elements, such as cross-laminated timber (CLT) constructions or hybrid concrete systems (e.g. screed-on-wood), do not necessarily behave like lightweight structures[3].

2   MODELLING BUILDING SOUND PROPAGATION

2.1. Empirical approach

Sound propagation models in building are empirical or involve sub-structuring. In an example of the former and to address structure-borne sound in inhomogeneous lightweight buildings, Schöpfer et al treat the whole building as a 'black box' to give the transmission function, the ratio of the sound pressure 'anywhere' in the building and an injected vibration power 'elsewhere' in the building[11]. Fig. 1 shows a selection of transmission functions for lightweight building systems. The injected power is measured as the cross-spectrum of the contact force and response velocity at an excitation point. The force was generated and recorded by an instrumented shaker (i.e. with in-line force transducer) or by an instrumented hammer, shown in Fig. 1(d). The response velocity is recorded using a matched pair of accelerometers about the excitation point. The transmission function is the level difference between spatial average sound pressure level (ref $2*10^{-5}$ pa) in the receiver room of interest and the spatial average power level (ref 10^{-12} W) over the excited wall/floor of interest. The transmission function is now defined and its measurement specified in the series EN ISO 10848[6].

Fig. 1 shows that the ensemble ranges are of the order of 10-20 dB. The trend curves are generally monotonic and point to simple functions of frequency. There is the potential to create data bases as simple prediction tools, and there are ongoing field measurements, and work on how building types could be grouped and classified.
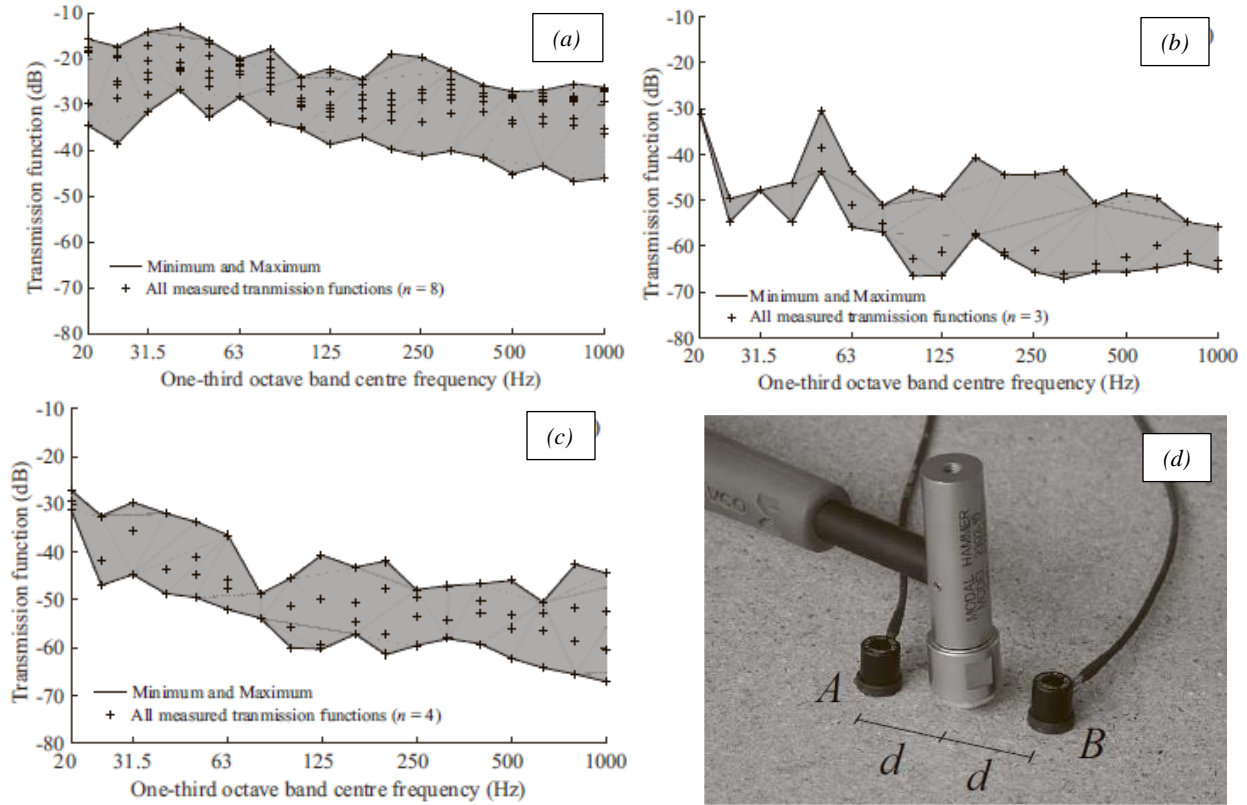
Fig. 1 - Field measured transmission functions: (a) horizontal transmission through plasterboard on timber wall; (b) diagonal transmission through the same wall above and below a timber-joist floor; (c) vertical transmission through timber-joist floor; (d) force hammer excitation with matched accelerometer pair, after [11].

2.2. Sub-structuring approach

In the alternative sub-structuring approach, the building elements (e.g. walls or floors), including junctions, are measured under laboratory conditions and then fictively joined to form the whole building. The sound propagation models are a reduced form of Statistical Energy Analysis (SEA)[12, 13], in that junctions between adjacent spaces only are considered[3, 4, 14].
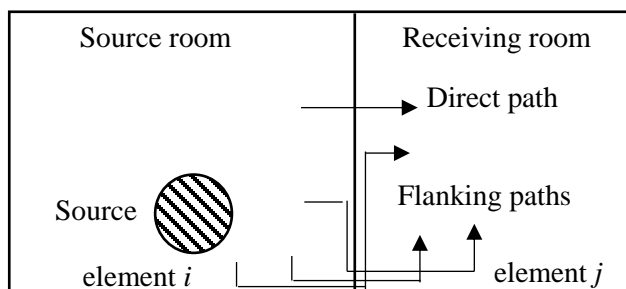

Fig. 2 – Direct and flanking paths for horizontal airborne sound transmission; for clarity, the flanking paths are only shown for one junction

Consider airborne sound transmission between horizontally adjacent rooms. The Standard ISO 12354-1 approach[3] is to consider each possible transmission path separately, shown in Fig.2, and then to sum their contributions. The procedures for transferring the laboratory data into *in situ* performance values are documented for heavyweight (Type A) constructions. Type A constructions are generally concrete floors and masonry walls, the junctions of which give a decrease in vibration level of less than 6 dB. Therefore the structural reverberation time at low frequencies is primarily determined by the connected elements. The following applies to the recently included lightweight (Type B) constructions[15, 16]. Type B constructions are generally of framed or ribbed plates of timber or other lightweight materials and the junctions have little influence on the structural reverberation time. For the direct path, the in-situ sound reduction index R_{situ} of the separating wall is obtained from laboratory measurement of sound reduction index R. For lightweight constructions there is no need to correct for loss factor, i.e. the ratio is of the reverberation times of the wall *in situ* and in the laboratory. According to ISO 12354-1[3], the flanking transmission path between element i in the source room and element j in the adjacent receiving room is characterized by R_{ij} defined as the sound power radiated by element j in the receiving room due to incident sound on element i in the source room and calculated from the performance of the elements along the path as

$$R_{ij} = \frac{R_i + R_j}{2} + \overline{D}_{v,ij,n} + 10log\left(\frac{S_S}{l_o l_{ij}}\right) dB \qquad (1)$$

$\overline{D}_{v,ij,n}$ is the normalized direction averaged junction velocity level difference, R_i, R_j the sound reduction index of element i and j (the walls are assumed bare for clarity) assuming resonant transmission only, using the element radiation efficiencies[3], S_S the surface area of the element separating the two rooms, l_{ij} the junction length and l_o a reference length ($lo = 1$m). Fig. 3 shows an example calculation of the horizontal transmission through a timber cavity wall where direct path and flanking contributions are shown.
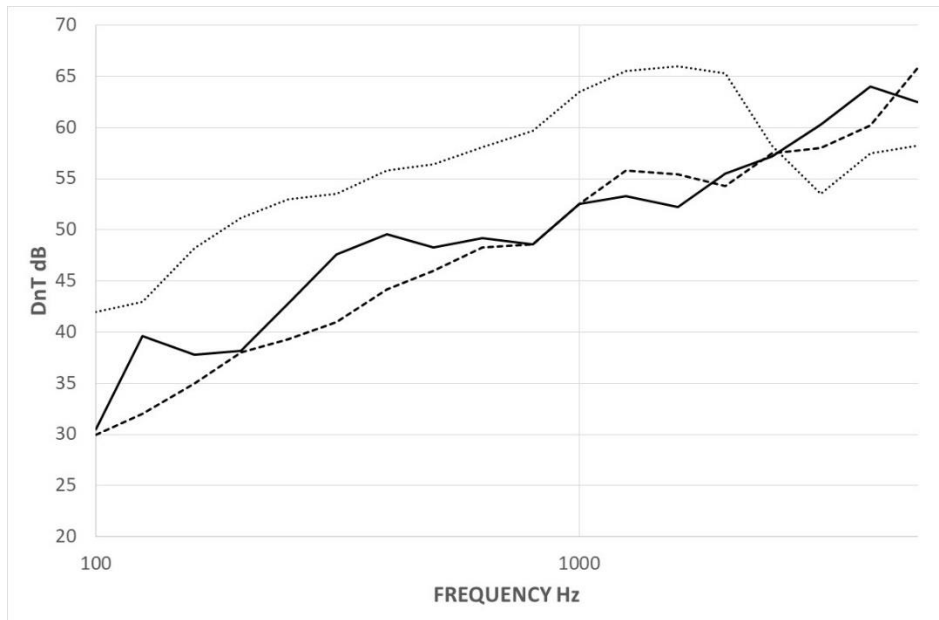

Fig. 3 - Sound insulation across a cavity wall with parallel floor joists: measured (solid line); laboratory measurement of wall alone (dotted line); predicted value including flanking paths (dashed line), after [15].

The coincidence dip, evident in the measurement of the wall alone, is not evident in the field measurement, showing that the timber cavity wall is probably not exactly the same as the one tested in laboratory. However, the example demonstrates that Standard methods are in place for predicting sound transmission in heavyweight and now in lightweight buildings; although obtaining the correct input data is not always straightforward.

For impact sound transmission, a similar sub-structuring approach is used as shown in Fig. 4, but where a reference active component (the well-known standard tapping machine) is on the floor of interest. According to the corresponding Standard ISO 12354-2[4], a flanking impact sound level $L_{n,ij}$ can then be defined as the sound pressure level radiated by element j in the receiving room generated by the tapping machine on element i in the source room; $L_{n,ij}$ can be calculated from the performance of the elements along the path, including the (direct) impact sound level $L_{n,i}$ of the impacted floor, measured in laboratory[4] with no flanking paths

$$L_{n,ij} = L_{n,i} + \frac{R_i - R_j}{2} - \overline{D}_{v,ij,n} - 10log\left(\frac{S_s}{l_0 l_{ij}}\right) dB \qquad (2)$$
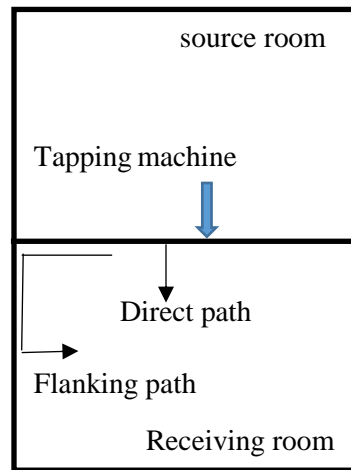

Fig. 4 – Direct and flanking paths for vertical impact sound transmission; for clarity, the flanking paths are only shown for one junction.

The sub-structuring approach, used for impact sound transmission, can be used for service equipment transmission[10]. The supporting building element i is characterized using a new quantity called unit power sound pressure level ($L_{ne,0,i}$) defined as the sound pressure level radiated in a laboratory with no flanking paths when a structure-borne sound source of unit power is connected to element i. From $L_{ne,0,i}$, the equipment sound pressure level $L_{ne,i}$ can be estimated using Eqn. (3), where the equipment contact power $L_{W,contact,i}$ is measured according to standard EN 15657[9], using the mobility approach described in Section 3

$$L_{ne,i} = L_{ne,0,i} + L_{W,contact,i} - L_{W0} \qquad (3)$$

L_{W0} is the unit power level in dB ref. 10^{-12} Watt ($L_{W0} = 120$ dB). The sound pressure level generated in-situ by any equipment connected to element i can therefore be obtained by using $L_{ne,i}$ as input

data in the prediction method for impact sound[4], i.e. by replacing $L_{n,i}$ with $L_{ne,i}$ in Eqn. (2) for any path ij. For lightweight buildings, the Standards[3,4] also suggest a semi-empirical approach, where each path ij is measured with the other paths shielded[6]. For impact sound transmission for example, the flanking impact sound level L_{nij} can be predicted from $L_{nij,lab}$ by only correcting for geometrical differences:

$$L_{n,ij} = L_{n,ij,lab} - 10log\left(\frac{S_i\, l_{ij,lab}}{S_{i,lab}\, l_{ij}}\right) \tag{4}$$

The same approach can be applied to service equipment. The tapping machine is replaced by a unit power structure-borne sound source, giving $L_{ne,0,ij,lab}$ and $L_{ne,0,ij}$, as in Eqn. (4).

3   SOURCE INPUT QUANTITIES

Airborne sound sources are characterized by their sound power W. A washing machine, compressor, fan unit, etc. can be described as a single frequency dependent value, typically in octaves or one third octaves, which can be input to a source-path-receiver model. Duct systems are spatially extended sources, which can be represented by localized airborne sound sources, which may be located along ducts (break-out) or at duct terminations. Airborne sound transmission to an adjacent room is then obtained using the sub-structuring approach[3], composed of flanking paths ij and using airborne sound power as source input data. The method assumes diffuse sound fields in rooms and only approximates the airborne sound power $W_{inc,i}$ incident to element i, discarding direct field and source directivity

$$L_{Winc,i} \approx L_W + 10lg(S_i/A_S) \tag{5}$$

S_i is the area of element i and A_S the equivalent absorption area of the source room. Eqn. (5) simply means that the ratio between source power (or power absorbed in the room) and the room equivalent absorption area is the same as the ratio between the power incident to element i and the area of this element, both being equal to the diffuse sound intensity in the room. The sound pressure level transmitted to the adjacent room through path ij is then readily obtained from $W_{inc,i}$ and R_{ij}, the ratio between power incident to element i in the source room and power radiated by element j in the receiving room. The total sound pressure level including all the paths ij is finally calculated for comparison with appropriate receiver (listener) criteria. There is a menu of standard recommended laboratory methods of obtaining the airborne sound power, including by source substitution, in reverberant conditions, in anechoic conditions and by intensity methods[6]. A significant simplification is possible because vibrating sources, which cause acoustic radiation, generally are not affected by fluid loading. Further, the mobility of the receiving system, or conventionally the impedance of the air, ρc, is assumed not to vary much with location, although in practice it depends on the closeness of the radiating surfaces to reflecting surfaces.

Concerning structure-borne sound sources (see Table 1), data for prediction are, or should be also expressed in terms of power, which now depends on the receiver properties. Pipe work and lift systems are spatially extended sources connected to different building elements, and can be replaced by localized structure-borne sound sources connected to these elements.

Table 1 – Airborne and structure-borne sound transmission in buildings

	Airborne	Structure-borne
Source input quantity	L_w	$L_{w,contact}$
Path	Room absorption Airborne sound insulation	Isolating mounts Structure-borne sound insulation
Design criteria Human response	L_{Aeq}, NC, RC Standards	L_{Aeq}, NC, RC Standards

4   STRUCTURE-BORNE SOURCES

The issue of structure-borne source characterization was raised by Kihlman[17] in a call for the development and standardization of measurement methods. In a response by ten Wolde and Gadefelt, several methods were proposed and considered[18]. The methods included measurement of the velocities or accelerations on the feet of resiliently mounted machinery (which eventually became a Standard[27]), measurement of an equivalent force by a substitution method, measurement of accelerations on a reception plate or of sound pressures in a reception enclosure. Gerretsen[19] considered the practicality of the proposed procedures, also Villot through case studies[20]. The primary consideration was on how such laboratory measurements relate to the performance of the machine when installed. Petersson and Gibbs assessed the methods according to the following criteria: a procedure should produce data which allows a comparison of sources, comparison with set limits, data for prediction and data for low-noise design[21]. The main conclusion, from reviews of the proposed methods[18] was that measurements should be on a power basis or transform to input power for when the source is installed.

Vibrating installations become structure-borne sources at supporting mounts, services runs and structural bracing. Multiple contacts generate multiple transmission paths but manufacturers and engineers desire a single value of source strength and it and the transmission should be expressed as powers[22, 23]. Three quantities are required for prediction of the transmitted power at an installation: source activity (either the free velocity or the blocked force of the operating machine), source mobility (or the inverse, impedance) and the receiver mobility (or impedance) of the supporting and connected structural element[24]. Fig. 5 gives the inverse analogous electric circuit of an active component connected to a passive receiver[25, 26], to give the contact force and contact velocity, the product of which gives the time-averaged power transmission at that contact. Y_S and Y_R is the source and receiver mobility, respectively. Mobility is the ratio of response velocity to applied force and is the inverse of impedance. Rotational components can be considered in terms of moment mobility, the ratio of angular velocity to applied moment.

The free velocity V_f is the velocity measured at each contact of the freely suspended source, operating under otherwise normal conditions[27]. The alternative for source activity, the blocked force (the force obtained at a contact with an inert receiver) previously required force transducers to be inserted at each contact with a heavy plate. This can alter the contact conditions. Recent work by Moorhouse et al[28] has circumvented this problem by measuring the blocked force as the ratio of contact velocity to the coupled mobility. This means that machines can be measured in situ. The method has the additional advantage in that it circumvents concerns that the internal mechanisms, which result in the free velocity at the connections, might be affected by disconnecting the device and resiliently supporting it.
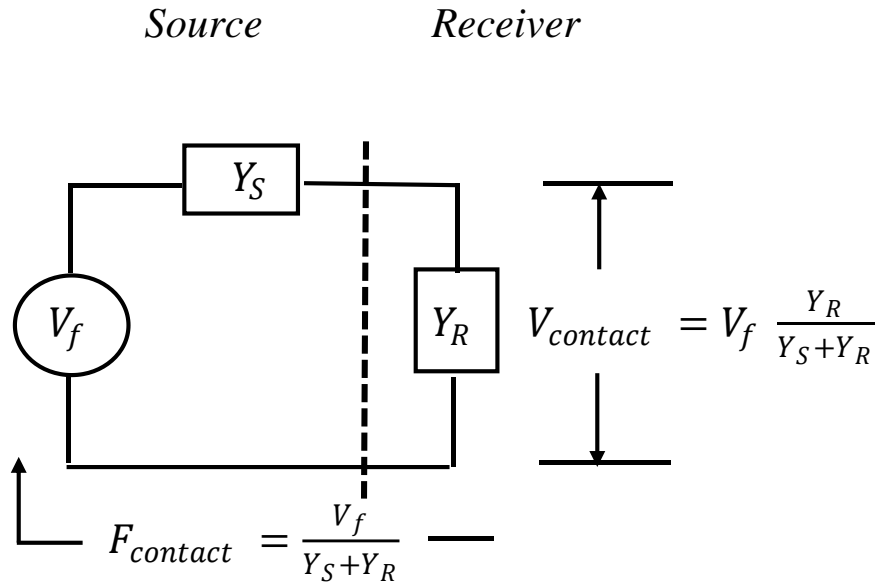
Fig. 5 – *Inverse analogous electric circuit of an active source connected to a passive receiver.*

The three source quantities are related

$$F_{blocked} = \frac{V_f}{Y_S} \qquad (6)$$

This relationship holds for single contacts and by matrix expressions for multiple contacts and degrees of freedom. Therefore, methods which give any two of the source quantities, then yield the third. In the following discussion, free velocity is considered as source activity. Whilst empirical methods have been developed for estimating the free velocity of fans[29], usually source activity is measured. The source mobility Y_S is complex and can be measured when the source is freely suspended. The supporting structure is represented by the receiver mobility Y_R. The transmitted power at the contact is the real part of the complex power, which is the product of contact force and contact velocity

$$P_{contact} = \frac{1}{2}|V_f|^2 \frac{Re(Y_R)}{|Y_S+Y_R|^2} \qquad (7)$$

Fig. 6 shows example magnitudes of source and receiver point mobility in buildings. For the example shown, the fan attached to a timber-frame or ribbed structure, the receiver mobility is significantly higher than the source mobility ($|Y_R|>>|Y_S|$) at frequencies below 125 Hz and below this frequency Eqn. (7) becomes the simpler expression

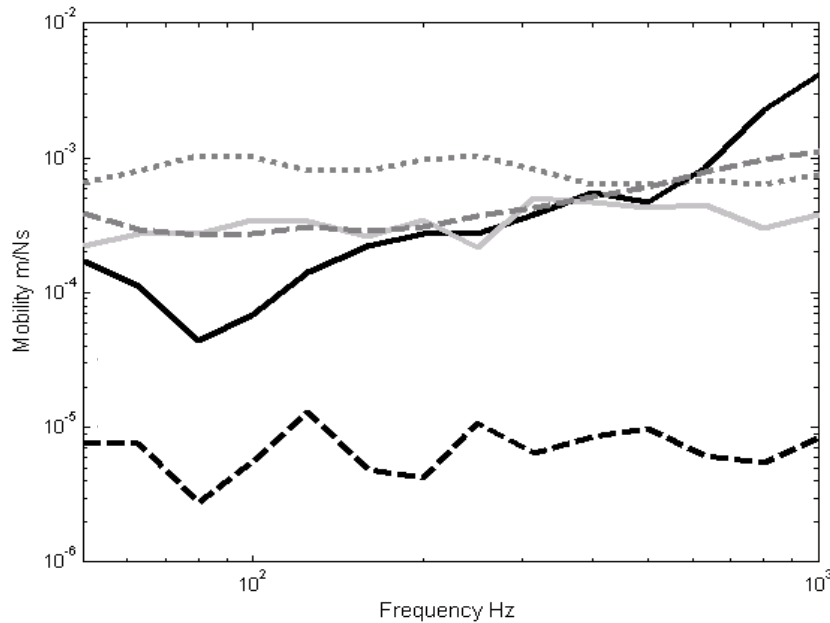$$P_{contact} \approx \frac{1}{2}|V_f|^2 \frac{Re(Y_R)}{|Y_R|^2} \qquad (8)$$

Fig. 6 - Magnitudes of point mobility at contact of: fan base (black line); whirlpool bath (solid grey); concrete floor (dashed black); timber frame/joist (dashed grey); chipboard (dotted grey).

This is the classic velocity source assumption. All that is required of the source is the measured free velocity squared. Measurement of free velocity at each contact is relatively straightforward[27], although there can be problems in ensuring that the machine operates normally. The squared quantity is real valued and therefore is measurable in frequency (e.g.1/3 octave) bands.

For the same fan and timber-frame/joist structure, above 800 Hz the receiver mobility is significantly lower than the source mobility ($|Y_S| >> |Y_R|$) and therefore, above 800 Hz, Eqn. (7) becomes:

$$P_{contact} \approx \frac{1}{2} |V_f|^2 \frac{Re(Y_R)}{|Y_S|^2} \approx \frac{1}{2} |F_b|^2 Re(Y_R) \qquad (9)$$

This is the classic force source assumption and the source is characterised by the blocked force squared. This assumption commonly applies to sources in heavyweight buildings. The sound pressure due to a force source is predictable using the Standard impact sound building propagation model[4]. The structure-borne sound pressure level is given by the predicted impact sound pressure level corrected for the difference in blocked force level between the source of interest and the standard tapping machine[30, 31]. The round robin results by Larsson and Simmons[32] are of practical interest, since the uncertainty of this simple method was not as large as anticipated. The application of the standardized tapping machine as a reference force source therefore could be of interest to practitioners dealing with structure-borne sound from service equipment mounted in heavy-weight structures. Fig.7 shows results for an impacted lightweight timber stair attached to a wall separating two rooms[30]. The predicted sound pressure level is shown from Eqn. (6) (blue line) and from Eqn. (9) (green line). The inaccuracies below 125 Hz are likely the result of the modal behaviour of the rooms, but where diffuse sound fields are assumed. Similar low-frequency inaccuracies occur in sound insulation predictions in general. The inaccuracies above 800 Hz indicate signal-noise problems in the measurements.
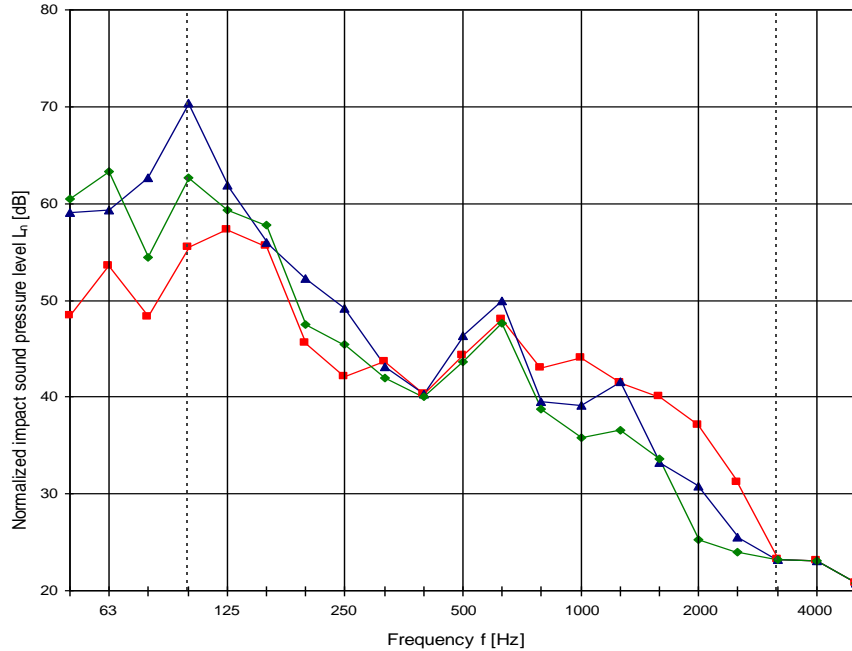
Fig. 7 - Measured sound pressure level in adjacent room due to a tapping machine on a timber stair (red); also predicted level from measured blocked force (green) and from free velocity and source mobility (blue), after [30].

The velocity source or force source assumptions seldom apply over the whole frequency range for sources in lightweight (e.g. timber frame/timber joist) buildings. Fig. 8 indicates the likely discrepancies if there is an incorrect assumption about the source-receiver mobility ratio[33].
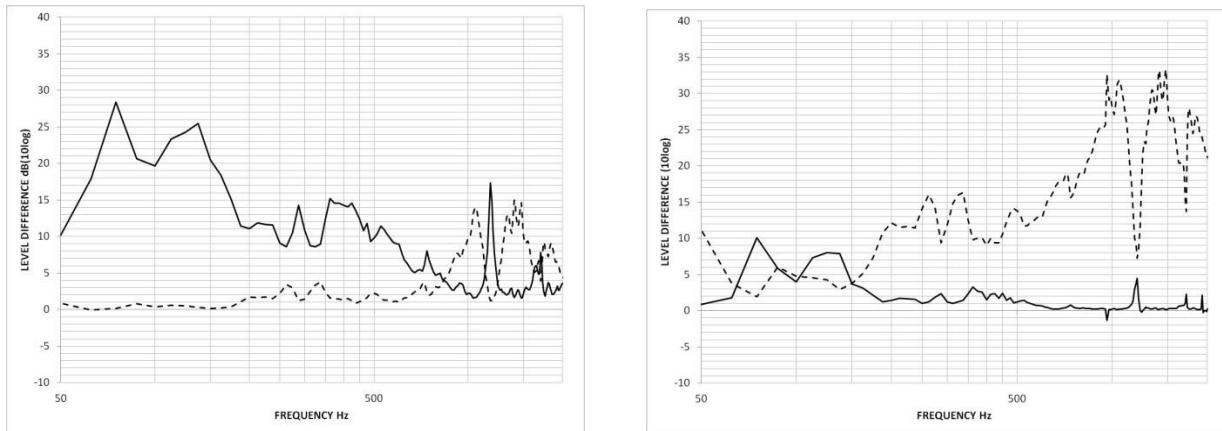

Fig. 8 – Ratio of estimated and calculated power for a force source (solid line) and velocity source assumption (dashed line) for a fan unit mounted on a lightweight building element (left) and on a heavier construction (right), after [33].

Referring again to Fig. 6, in the frequency range 200 – 500 Hz, the fan mobility is of the same order as that of the timber joist ($|Y_R|=|Y_S|$). Maximum power occurs when the source and receiver mobilities are complex conjugate[22, 23], but such matching conditions seldom occur or only in narrow frequency bands. The complex denominator in Eqn. (7) is assumed replaceable with the associated magnitudes and

$$P_{contact} \approx \frac{1}{2}|V_f|^2 \frac{Re(Y_R)}{|Y_S|^2 + |Y_R|^2} \tag{10}$$

This points to a significant simplification: all quantities in Eqn. 10 are real-valued and can be expressed as frequency-band averages favoured by engineers and consultants.

4.1 Isolators

What of the role of vibration isolators? Using the same convention for transmitted power through a rigid connection in Eqn. (7), the power transmitted through the isolator(s) becomes[34]

$$P_{isolator} = \frac{1}{2}|V_f|^2 \frac{Re(Y_R)}{|Y_S + Y_I + Y_R|^2} \tag{11}$$

Y_I is the isolator mobility. Using the same reasoning to obtain Eqn. (10), Eqn. (11) is replaced by

$$P_{isolator} \approx \frac{1}{2}|V_f|^2 \frac{Re(Y_R)}{|Y_S|^2 + |Y_I|^2 + |Y_R|^2} \tag{12}$$

This simplification does not apply near resonance frequencies of the system, since phase becomes important. The ratio of Eqn. (12) to Eqn. (10) is the isolator insertion loss on a power basis

$$\frac{P_{isolator}}{P_{contact}} \approx \frac{|Y_S|^2 + |Y_R|^2}{|Y_S|^2 + |Y_I|^2 + |Y_R|^2} \tag{13}$$

In Table 2 are some idealized installation conditions, assumed independent of frequency for clarity.

Table 2 – Isolator insertion loss for various installation conditions

Installation	Y_S m/sN	Y_I	Y_R	Isolator insertion loss dB
On concrete floor	10^{-4}	10^{-2}	10^{-5}	40
On timber joist	10^{-4}	10^{-2}	10^{-4}	37
On bay between joists	10^{-4}	10^{-2}	10^{-3}	20
Compliant machine base on bay	10^{-3}	10^{-2}	10^{-3}	17
Very compliant base on bay	10^{-2}	10^{-2}	10^{-3}	3

For the source on a thick concrete floor, Eqn. (13) gives a theoretical (and optimistic) reduction in power of 40 dB due to the introduction of the isolator (using the 10log convention). For the same source and isolator on a bay between timber joists, the power reduction is 20 dB. For a very compliant machine base, the previous case gives a reduction of 3 dB. The disappointing performance is because the very compliant machine base is already behaving as an isolator and the

added isolator has relatively little effect. Again, these estimates are not precise, since the complex values of mobility, and the resultant phase relationships, have been ignored. However, the simple expressions illustrate the dependence of isolator performance on all three mobilities and all must be known, in some form, for installations in lightweight building structures.

This paper now concentrates on rigidly attached machines and isolators are not considered further. Predicted sound pressures, due to rigidly attached machines, provide bench mark estimates of the remote sound pressure levels for comparison with room criteria. The isolator performance can then be specified on a power basis, with respect to achieving the room criteria.

4.2 Multiple components and contacts

Service equipment and other devices are attached to supporting structures through multiple contacts. At each contact, up to six components of excitation and response are possible. Three of the six components of excitation can be neglected a priori: torsions about axes perpendicular to the receiver surfaces, and forces parallel to the receiver surfaces. Whilst moments about axes parallel to the receiver surfaces can assume importance at high frequencies and/or at locations close to junctions, they generally can be neglected in buildings[35, 36]. Fig. 9 shows the moment induced powers, normalised by the power from forces perpendicular to the receiver surface for a fan unit on a timber-joist floor[37]. The force-induced power is generally dominant and moments and rotational velocities can be neglected. This points to the simplifying assumption that vibrating sources in buildings can be assumed to generate forces perpendicular to the receiving surfaces only. This may not be true in more 'carefully engineered' structures (e.g. aircraft, submarines, vehicles, etc.).
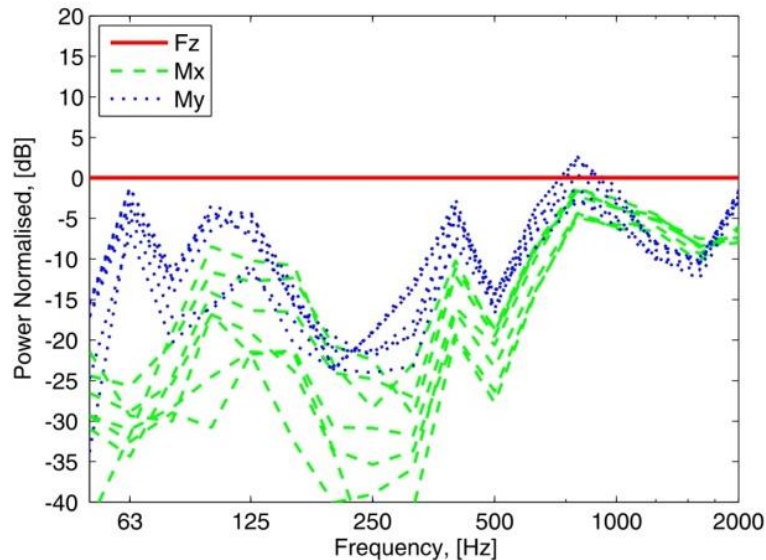

Fig. 9 - Power of the moment components, normalised with respect to the power of the perpendicular force components, for ten locations of a fan unit on a timber joist floor, after [37].

For multiple contact sources, the total transmitted power consists of point contributions and transfer contributions between contacts. Fig. 10 shows point and transfer mobilities of a whirlpool bath with eight mounts (left) and of a fan unit with four mounts (right). The magnitudes of transfer mobility generally are less than those of the point mobility. This points to the final simplifying assumption: equivalent single values of source and receiver mobility can be expressed as averages of the point mobility over the contacts. This simplification is expressed with some caution since

the total power transmission is a complex combination point and transfer terms, where the phase relationships between the contact forces might be influencial[38, 54] and more research is required.
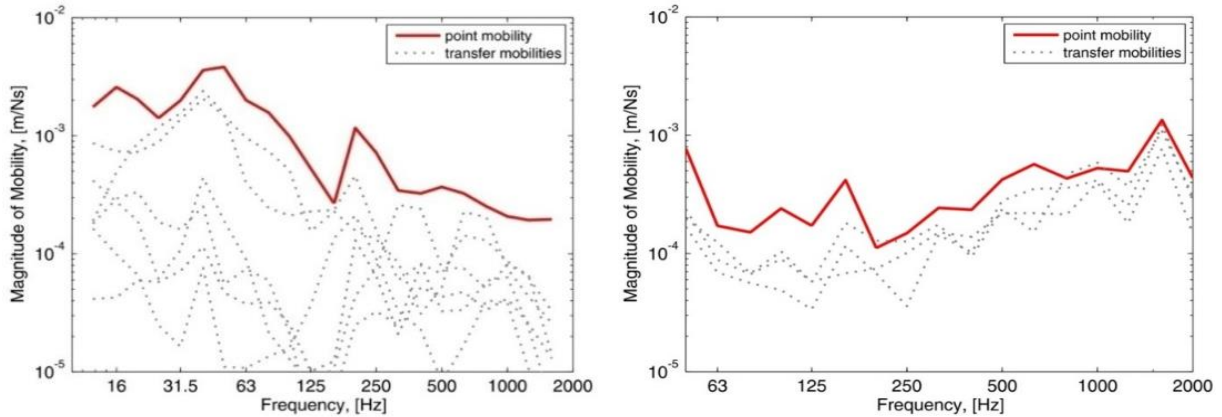

Fig. 10 - Transfer mobilities (dotted lines) between eight mounts of a whirlpool bath (left); between four fan mounts (right), after [38].

To summarise, the vibrational activity of structure-borne sound sources in buildings can be measured as the sum of the squared free velocity over the contacts, or the sum of the squared blocked forces. The source mobility is expressed as the average point mobility magnitude over the contacts. For the transmitted power, the required real part and magnitude of the receiver mobility is also expressed as average values over the contacts or as spatial averages over the area of the building element. All quantities are frequency band averages.

What of sources connected to more than one building element, such as in a corner location? Fig. 11 shows that equipment can energise a floor and two walls simultaneously, with vibration energy flow between elements. In these cases, the equipment is treated as three sources in the same way as described for a source on a single receiver. This requires three sum squared free velocities and three average point mobilities. The resultant three transmitted powers are input into the Standard propagation models[3, 4] and the path contributions summed on an energy basis[39].
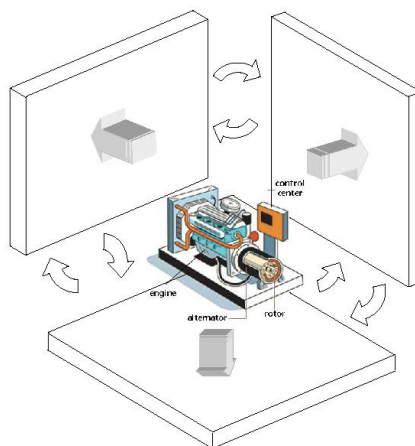

Fig. 11 – Simultaneous power transmissions into three building elements from a source in a corner.

5 SINGLE STAGE AND TWO STAGE RECEPTION PLATE METHODS

5.1 Principle of the method

Laboratory measurements of structure-borne source quantities should be with reference to the likely receiver characteristics in buildings. Most building elements are plate-like. Heavyweight elements are homogeneous with monolithic junctions: e.g. concrete floors and floating floors, concrete and masonry walls. Lightweight elements are framed or ribbed plates: e.g. plasterboard and studding cavity walls, timber-joist floors. Cross laminate timber (CLT) constructions can be treated as heavyweight elements. Laboratory procedures have been developed, which incorporate plate-like reception rigs, to which the sources under test are attached[9].

The principle of the reception plate method is based on statistical energy analysis (SEA)[12]. The total transmitted power of often complicated and extended sources is equal to the resultant total energy loss in a connected simple plate receiver. It is assumed that the total plate energy is contained in the bending field. Whilst SEA normally requires that the plate bending field has a high modal density[31], it has been shown that the power equality holds for thick plates of low modal density[38, 39]. The reception plate method (RPM) requires the operating source to be attached to a plate, which is isolated from the laboratory floor. The plate response velocity is sampled using accelerometers distributed about the plate. Fig. 12 shows a whirlpool bath with eight mounts, on a resiliently supported 100 mm concrete reception plate. The total power from the source through all contacts equals the plate energy loss, calculated from the plate parameters.

$$P_{source} = P_{plate} = \omega \, \eta \, M \left\langle v^2 \right\rangle \qquad (14)$$

$\langle v^2 \rangle$ is the mean-square reception plate velocity when the source is in operation, η is the total loss factor of the plate (of mass M), obtained by the decay method.
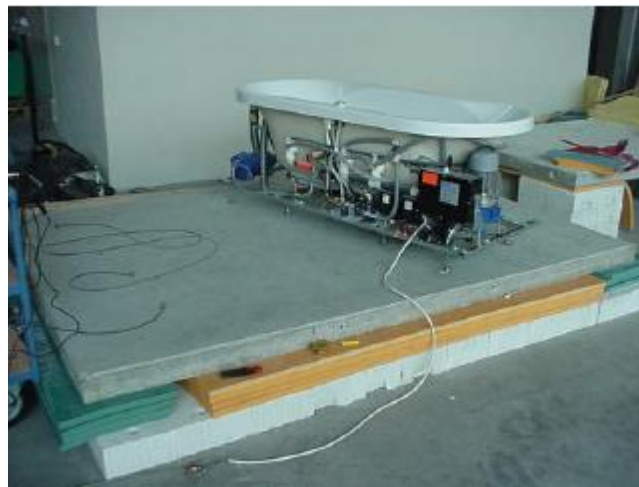

Fig. 12 - Whirlpool bath on a resiliently supported 100 mm concrete plate, after [38, 39].

Alternatively, and when the reception plate is not isolated (e.g. heavyweight walls and floors in buildings), a power substitution method can be applied. An instrumented shaker or hammer provides the cross-spectrum of the applied force and acceleration at the contact to give the input power and distributed accelerometers give the mean square plate velocity. Replacing the shaker or

hammer with the source under test and measuring the mean square plate velocity again gives the source power[30, 40].

The link between RPM measurement and the power expression is seen by combining Eqn. (10) with Eqn. (14)

$$\frac{1}{2}\left|V_f\right|^2 \frac{Re(Y_R)}{|Y_S|^2 + |Y_R|^2} \approx \omega\eta M\langle v_{plate}^2\rangle \qquad (15)$$

Eqn. (7) to Eqn. (10) demonstrate that two source quantities are required for prediction of the power when the source is installed in buildings or other structures. This points to the use of the reception plate method to obtain the two quantities. If the reception plate mobility is much higher than source mobility, then from Eqn. (15) and Eqn. (8), a single source quantity is obtained, related to the sum square free velocity over the source contacts[41, 42]

$$V_{RPM}^2 \approx \Sigma_i^N\left|V_{fi}\right|^2 \qquad (16)$$

Likewise, if the reception plate mobility is much lower than the source mobility, then from Eqn. (15) and Eqn. (9), a single source quantity is obtained, related to the sum square blocked force over the same contacts

$$F_{RPM}^2 \approx \Sigma_i^N|F_{bi}|^2 \qquad (17)$$

When both V^2_{RPM} and F^2_{RPM} have been measured (i.e. by the two-stage method), an equivalent single source mobility is obtained, which approximates the average point mobility over the contacts.

$$Y_{SRPM} = \sqrt{\frac{V_{RPM}^2}{F_{RPM}^2}} \approx \frac{1}{N}\Sigma_i^N|Y_{Si}| \qquad (18)$$

The equivalent single source quantities are combined with measured or calculated receiver mobility, to predict the structure-borne power into any other plate-like supporting structure of mobility Y_R

$$P_{RPM} \approx \frac{1}{2} \frac{V_{RPM}^2 Re(Y_R)}{Y_{SRPM}^2 + |Y_R|^2} \qquad (19)$$

Table 3 shows the two-stage method, indicating alternative direct and RPM measurements. The method yields source data for calculation of the transmitted power for any source-receiver mobility ratio installation. There are alternative routes through the procedure indicated in Table 3. For a simple source such as a fan or motor on four mounts, it may be easier to measure the sum square free velocity directly. For a more complicated source on many mounts, it may be more convenient to conduct a RPM measurement on a thin reception plate.

Table 3 – Reception plate method (RPM) and direct methods for prediction of installed power. .

Quantity	Direct measurement	RPM measurement	For predicted power
Free velocity	$\|V_{fi}\|$ at contacts for $\sum_i^N \|V_{fi}\|^2$	$V_{RPM}^2 = \dfrac{2P_{high\ mob}}{Re(\frac{1}{Y_{high}})}$	Either value since $$V_{RPM}^2 \approx \sum_i^N \|V_{fi}\|^2$$
Blocked force	$\|F_{bi}\| = \dfrac{\|v_{fi}\|}{\|Y_{Si}\|}$ at contacts for $\sum_i^N \|F_{bi}\|^2$	$F_{RPM}^2 = \dfrac{2P_{low\ mob}}{Re(Y_{low})}$	Either value since $$F_{RPM}^2 \approx \sum_i^N \|F_{bi}\|^2$$
Source mobility	$\|Y_{Si}\|$ at contacts for $\dfrac{1}{N}\sum_i^N \|Y_{Si}\|$	$Y_{SRPM} = \sqrt{\dfrac{V_{RPM}^2}{F_{RPM}^2}}$ $or = \sqrt{\dfrac{\sum_i^N \|V_{fi}\|^2}{F_{RPM}^2}}$	Either value since $$Y_{SRPM} = \dfrac{1}{N}\sum_i^N \|Y_{Si}\|$$
Receiver mobility	$Re(Y_R) = \dfrac{1}{N}\sum_i^N Re(Y_{Ri})$ $\|Y_R\| = \dfrac{1}{N}\sum_i^N \|Y_{Ri}\|$		$$Re(Y_R) \approx \| Y_R\| \approx Y_{char}$$
Installed power	$P_{instal} = \langle v_{instal}^2 \rangle P_{cal} / \langle v_{cal}^2 \rangle$		$P_{RPM} \approx \dfrac{1}{2}\dfrac{V_{RPM}^2\, Re(Y_R)}{Y_{SRPM}^2 + \|Y_R\|^2}$ or $\approx \dfrac{1}{2}\dfrac{\sum_i^N \|V_{fi}\|^2\, Re(Y_R)}{Y_{SRPM}^2 + \|Y_R\|^2}$

How are the two source-reception plate mobility ratios achieved without prior knowledge of the source mobility? This problem is circumvented by designing reception plates with mobilities outside the range of likely source mobilities. Fig. 4 and later, Figs. 18-20, indicate that a high mobility reception plate of mobility 10^{-2} m/sN would be suitable and is achievable with 1-2 mm thickness aluminium or steel sheets, for example. A low mobility reception plate of mobility 10^{-5} m/sN would be suitable and is achievable with 100 mm thickness concrete.

Fig. 13 shows some typical results, for a compact air pump attached to a ribbed plate, representative of an installation on an airplane[43]. Fig. 13 (lower) is of particular relevance to manufacturers of isolation systems, since it shows predicted in-situ performance and the ratio of

predicted isolated to un-isolated performance is the insertion loss of their product on a power basis and in an installed situation.
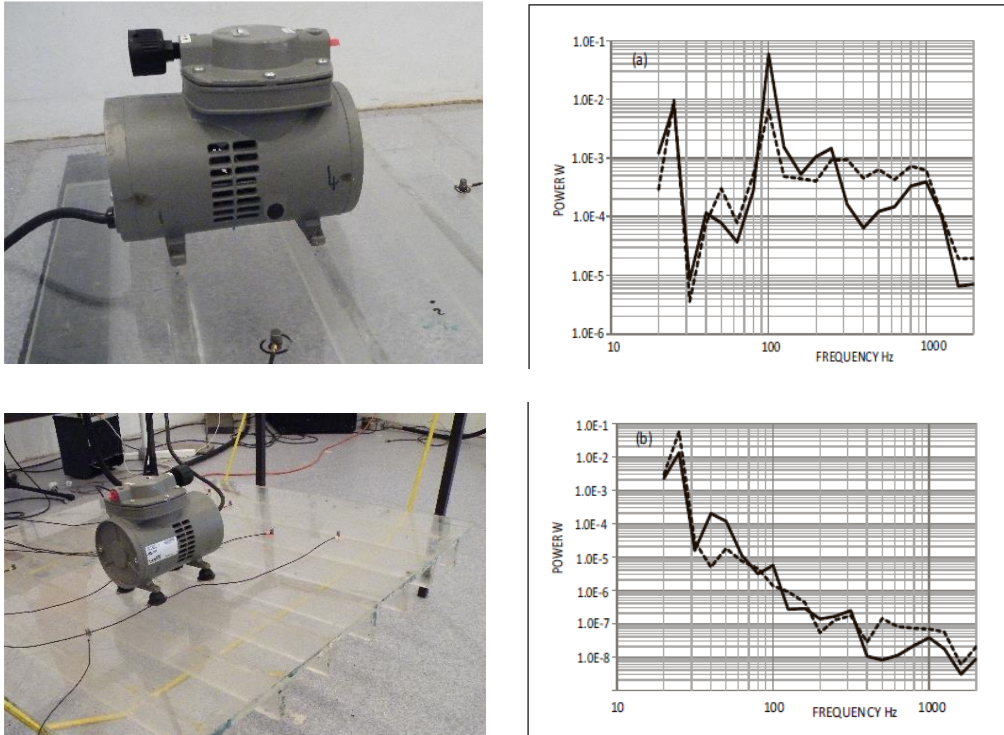

Fig. 13 - Measured transmitted power (solid line) and from RPM prediction (dashed), for a rigidly connected air pump on a ribbed plate (upper curve) and through isolators (lower), from [43].

An example of the application of this approach to buildings[44] is given for a medium-size fan on a timber joist floor, in Fig. 14. The free velocity was measured directly and the blocked force from the RPM on a low mobility 20mm aluminum reception plate. The real part and magnitude of the receiver mobility were measured directly at floor locations over joists and in bays.

Fig. 14 - Fan, resiliently suspended in laboratory; timber joist chipboard floor under construction.

Fig. 15 (left) is the combined direct/RPM estimate of the fan power through four mount points at one location on the joist floor compared with the power calculated by the mobility method, also

(right) through four mount points at ten locations on the timber joist floor normalized with the calculated value at each location. On average, the RPM estimate is within 2 dB of the calculated value, with deviations of 4 dB above 800 Hz.
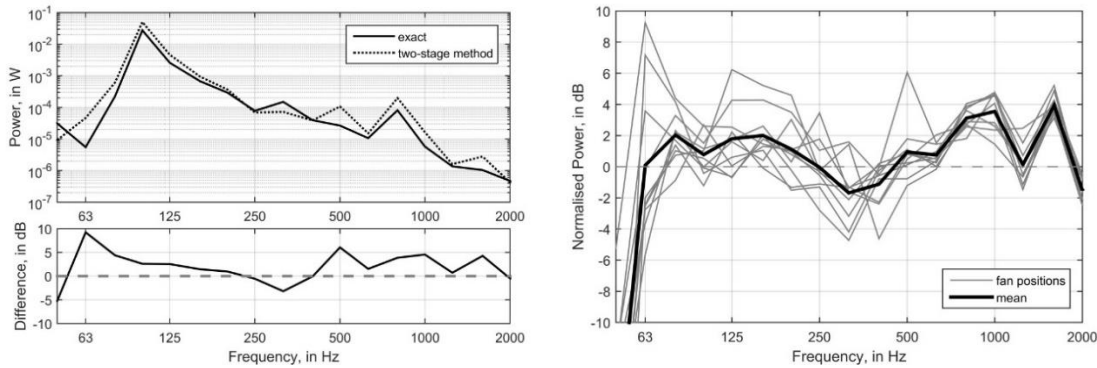
Fig. 15 - Transmitted power for fan located with two contacts on a joist and two contacts in adjacent bay (left); normalised power at ten fan positions with average value (right), from [44].

5.2   Uncertainty of the RPM

Methods of data reduction, such as by the RPM described, have inherent uncertainties[45]. The probabilistic approach to the steps in the two-stage method[46] show that if the errors in input values are 1 dB (i.e. in the terms $P_{high\ mobility}$, $R(1/Y_{high\ mobility})$, $P_{low\ mobility}$, $R(Y_{low\ mobility})$ and the receiver mobility in Table 3), then the error in the predicted transmitted power is 4.5 dB. For input errors of 3 dB, the error in predicted power is 7 dB. Using sample standard deviations of each step of the two-stage method[43] shows that for a compact source, the uncertainty in the estimate of source mobility ranged from 8 dB at low frequency to 6 dB at high frequency. For an extended source, the uncertainty also ranged from 8 dB to 6 dB.   Scholl calculated uncertainties in the estimate of source mobility of about 10 dB for domestic objects set down or dropped and which could not be measured directly[47]. Wittstock considered walking persons, shower jets and piped water systems[48]. The uncertainty in structure-borne sound powers from shower jets was 10 dB at 50 Hz, reducing to 5 dB at 500 Hz and 3 dB at 4 kHz. Vogel et al applied the two-stage method to several common sources: compressor, fan, extractor hood and shaker, when attached to various light and heavy plate structures[49]. The level differences between measured and two stage estimates were +/- 5 dB on average.

More work is required on the uncertainty of the two-stage RPM (or combined direct/RPM) and on indirect methods in general. From the authors' personal experiences, the uncertainty may be expected to be: +/- 10 dB below 80 Hz; +/- 5 dB between 80 Hz and 400 Hz; +/- 3 dB above 400 Hz. More measurement case studies are required however and an on-going Round Robin test, based on testing the same reference source using standard EN 15657[9] in several laboratories in Europe, will give clearer indications of the precision.

6.   CALCULATED SOURCE AND RECEIVER MOBILITIES

It is not likely that the receiver quantities, required for predicting structure-borne power, will be measured prior to the installation of mechanical installations. The required receiver quantities are the average real part and average magnitude of point mobility, over the contact points with the

source of interest, or the spatial averages over the building element area. Also for sources, calculation methods may provide convenient alternative estimates, which can be used to check and understand measurement results. Free velocity or blocked force must be measured, however.

6.1 Receiver mobility

6.1.1 Heavyweight building elements

Heavyweight walls and floors are mainly of concrete or masonry construction. Whilst displaying modal behaviour, particularly evident at low frequencies, peak values of the point mobility are difficult to predict, since the modal behaviour depends on source location and the edge conditions, neither of which will be known precisely prior to location of the mechanical or water installation. However, statistical estimates can suffice. Of relevance is the concept of the characteristic mobility[31], which is the mobility of an infinite plate of the same material and thickness as the wall or floor of interest, given by

$$Y_{char} = \frac{1}{8\sqrt{B'm'}} \qquad (20)$$

m' is the mass per unit area and $B' = \dfrac{Eh^3}{12(1-\mu^2)}$ is the bending stiffness for modulus of elasticity E, Poisson's ratio μ and plate thickness h. The characteristic mobility is frequency invariant and is real-valued. Fig. 16 shows measured point mobility at seven locations on a dense concrete plate (left) and on an aerated concrete plate (right). Both were free plates on resilient pads. Also shown is the characteristic mobility (horizontal line) for both cases. As expected, the dense concrete has a lower mobility than the aerated concrete.
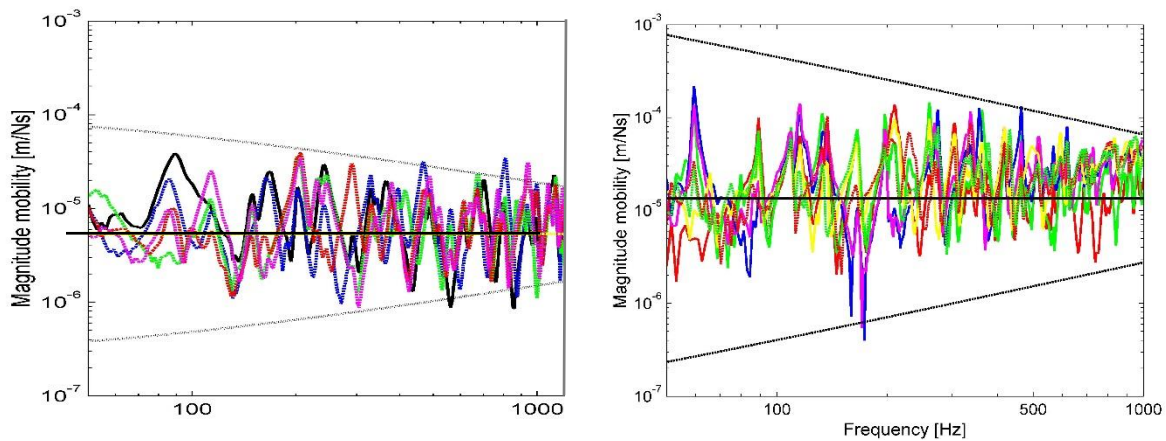
Fig. 16 - Point mobility at 7 locations on concrete plate (left) and on aerated concrete plate (right), from [50].

Whilst the modal peaks and dips in point mobility are difficult to predict, limits (shown) are easier to estimate[51]

$$Y_{max} = Y_{char} coth\left(\frac{1}{\beta}\right); \quad Y_{min} = Y_{char}/coth\left(\frac{1}{\beta}\right) \qquad (21)$$

$$\beta = 4/(\omega \eta M Y_{char})$$

The limits depend on mass M and loss factor η, which are relatively easy to estimate. The upper limit leads to an upper limit to the installed structure-borne power of a source, which is of importance.

6.1.2 Lightweight building elements

Lightweight building elements, found in timber-frame constructions for example, are not homogeneous and the receiver mobility varies significantly with location, particularly between when over structural reinforcement (e.g. joists or timber frames) and when in a bay (e.g. when attached to sheathing). Fig. 17 shows the results of a survey of point mobility measurements at random locations on 15 timber-frame constructions, including over joists and frames and in bays between joists or frames[52]. Shown is the mean value of point mobility and standard deviation. The point mobility of lightweight building elements has a mean value of the order of 10^{-3} m/Ns. The highest values occur on single layers of plasterboard sheathings on metal stud walls. The lowest values occur at fixings between plates and joists/frames.
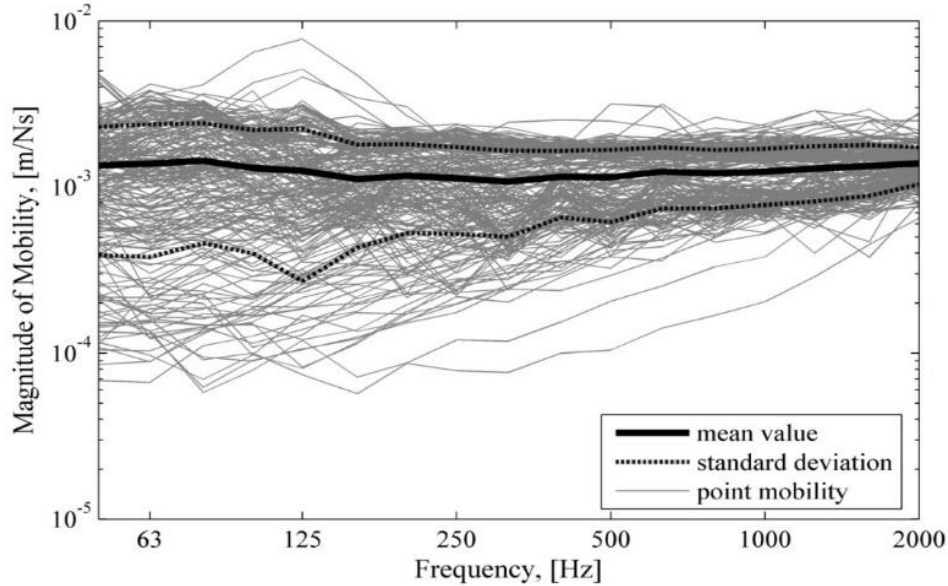
Fig. 17 – Mean and standard deviation of mobility of 15 timber constructions, after [52].

The mobility at the fixing points on frames or ribs can be approximated by the complex characteristic beam mobility[31]

$$Y_{beam} = \frac{1}{2m'c_B(1+j)} \qquad (22)$$

where c_B is bending wave velocity and m' is the mass per unit length. The two main components of an inhomogeneous lightweight building element, the frame/rib and the sheathing, can be incorporated into a mobility curve, related to the distance from the frame/rib. Fig. 18 shows the

measured point mobility over a timber-joist floor. Beam behaviour is evident at low frequencies and at short distances from the fixing between the sheathing and support. With increased distance and increased frequency, the mobility tends to the characteristic plate mobility of the sheathing. The real part of the measured mobility is normalised with respect to that of an infinite plate and plotted as a function of distance from a fixing point, normalised with respect to the governing bending wavelength in the sheathing. Beam-like behaviour is evident at low frequency and plate-like behaviour at high frequency, with a monotonic increase in the transition region. Such simplified methods are likely to suffice for the needs of building acoustics.
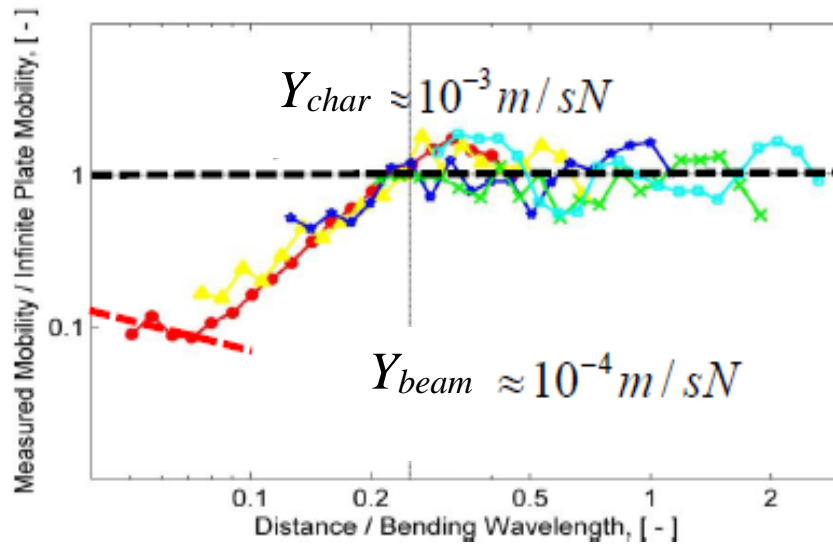
Fig. 18 - Real part of normalised point mobility, as function of normalised distance to fixings, [52].

6.2   Source mobility

Building services installations are more complicated, with a wider range of contact geometries, than for building elements. However, the mobility at the contact points is dictated by the material and geometry of the machine base around the contact. On this basis, machine bases may be categorised as either: compact, plate-like, flange/cantilever, frame[53].

6.2.1   Compact sources

Compact sources, such as domestic circulation pumps and small electric motors behave as rigid masses at low frequencies. The expression for rigid body mobility is

$$Y_{rigid} = \frac{1}{j\omega}\left(\frac{1}{M} + \frac{y^2}{I_{xx}} + \frac{x^2}{I_{yy}} \right)$$

(23)

where x, y are the distance coordinates of the contact point of interest from the centre of gravity of the source and I_{xx} and I_{yy} are the moment of inertias about the x and y axis, respectively. In Fig. 19

is shown the mobility at two points on a small air pump with short cantilever mounts. Rigid body behavior occurs up to 300 Hz. Between 300 Hz and 2500 Hz the cantilevered mounts flex and the mobility is stiffness controlled with magnitude

$$Y_{stiffness} = \frac{4\omega L^3}{Ewh^3} \qquad (24)$$

L, w and h are the length, width and thickness of cantilever, respectively; *E* is the elastic modulus. Above 2500 Hz, the mobility is resonance controlled and described by the characteristic beam mobility in Eqn. (22). The measured mobilities are in narrow frequency bands, with peaks and dips clearly indicated, but the predicted trend lines provide a practical estimate for each of the three frequency regions of dynamic behavior. In the following, the measured source mobilities are presented as averages of the point mobilities, for comparison with predictions.
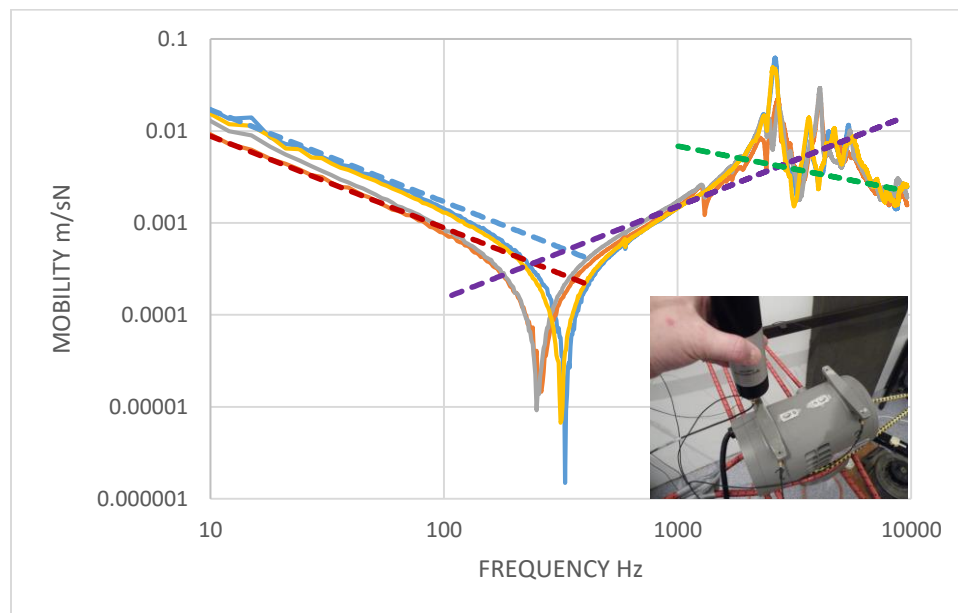
Fig. 19 - Measured point mobility of a compact air pump and calculated values.

6.2.2   Plate-like machine bases

Plate-like machine bases provide a platform for, e.g., fan units with separate electric motors. The plate-like behavior mirrors that for receiver building elements, already described. Fig. 20 shows the point mobility at four mounts of a fan plate base, with the characteristic mobility indicated. The measured narrow-band values show sharp peaks and dips, which reduce when presented as octave or third octave values and the characteristic mobility can be assumed representative.
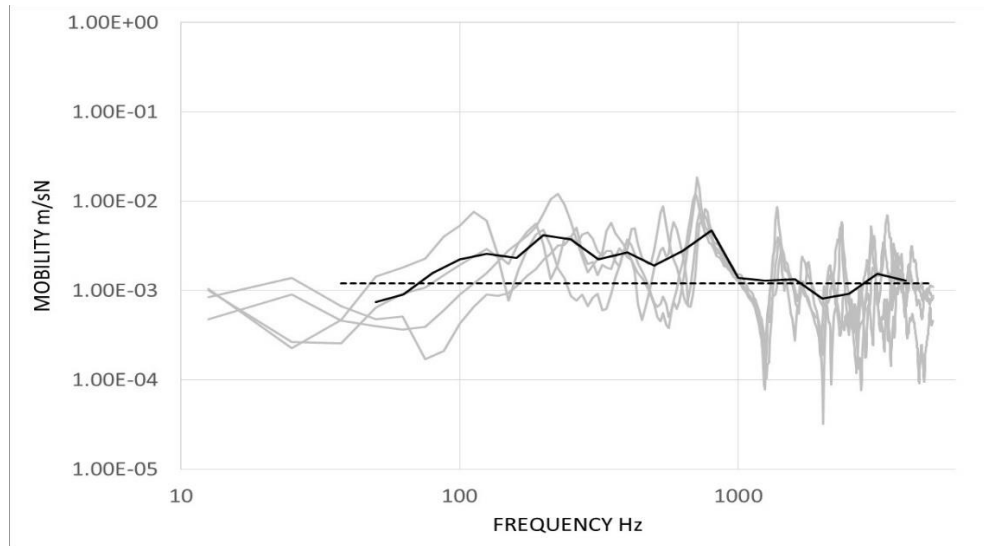
Fig. 20 - Point mobility at four mounts on a fan plate base: average in third octaves (solid black line); characteristic mobility (dashed line)

6.2.3   Flange-cantilever machine bases

Fig. 21 is of the mobility of a flange base, i.e. cantilevered along long edges. Rigid body behavior occurs below 80 Hz. Between 80 Hz and 1 kHz, the mobility is stiffness controlled. Above this region, the mounts behave as a resonant plate. These calculations are less accurate than those of Petersson and Plunt[54], since resonant peaks and dips are not indicated, but they provide estimates of source mobility appropriate for predicting structure-borne power transmission in buildings.
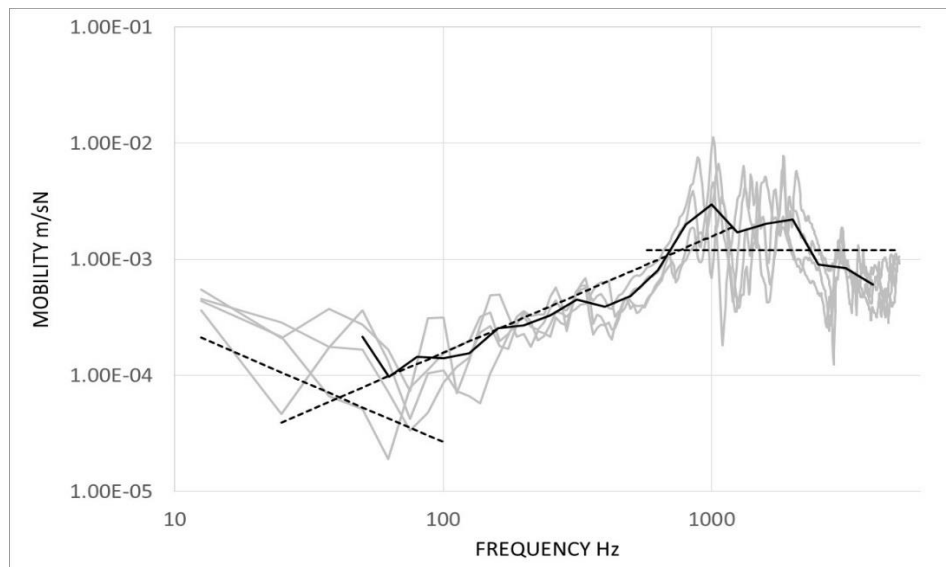
Fig. 21 - Point mobility at four points on a fan flange base: average in third octaves (solid black line); estimate (dashed line)

6.2.4   Frame bases

The mobility of frame bases varies significantly with mount point, since contact geometries (distances from free ends to frame junctions, overlapping framing, etc.) differ greatly. In Fig. 22 is

shown the mobility at eight mount points of the base frame of a whirlpool bath. For the example shown, the measured values converge to the characteristic beam mobility of the rectangular section frame. The characteristic beam mobility corresponds to the average point mobility, but it is likely that more detailed modelling is required to construct mobility curves for frame bases.
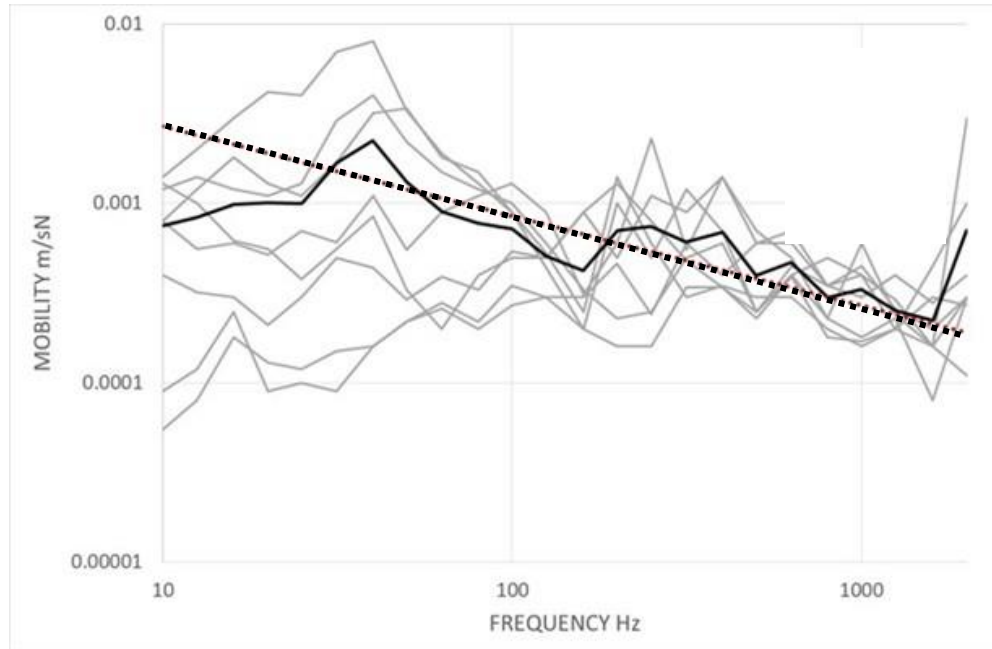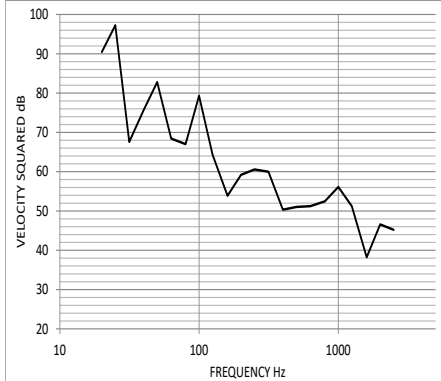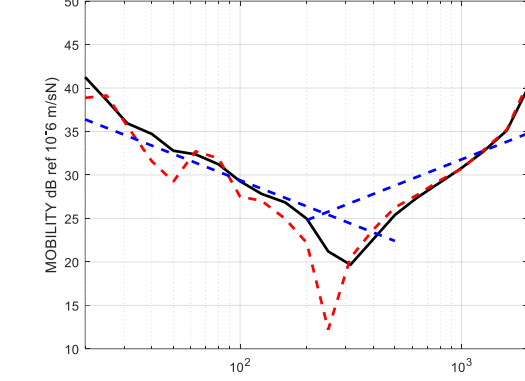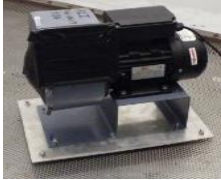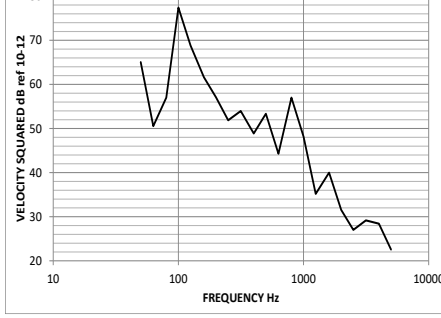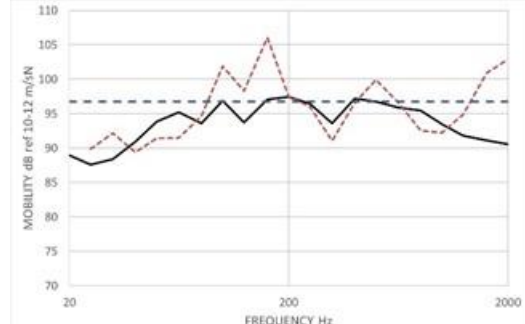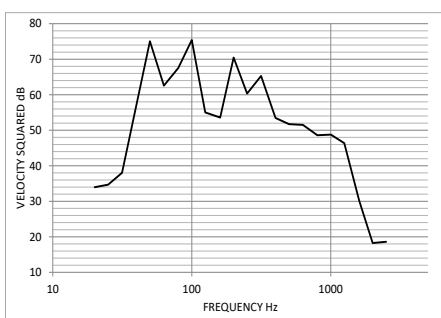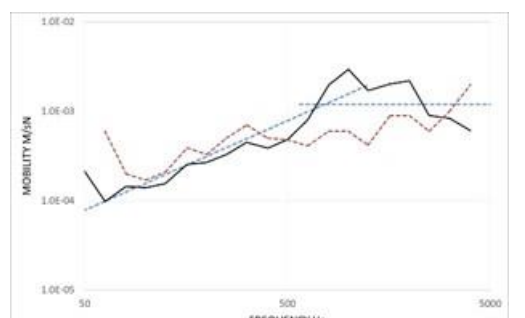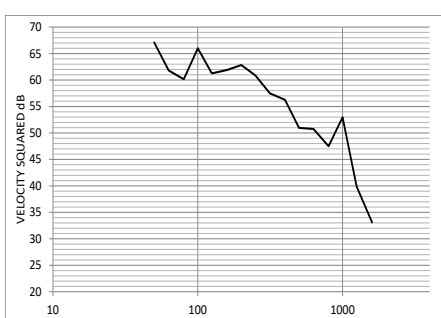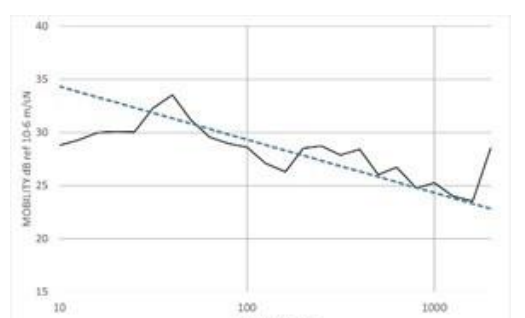

Fig. 22 - Point mobility at eight mount points on a frame base with average value (black line) and characteristic beam mobility (dashed line)

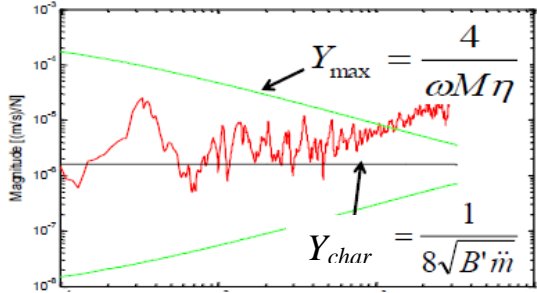## 7   DATA BASES FOR PREDICTION
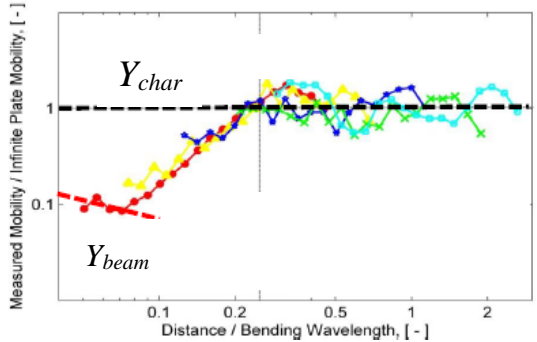
This section considers how a data base might be assembled for consultants and engineers, requiring methods of predicting structure-borne sound in buildings as straightforward as for airborne sound. Table 4 shows source data as single-value quantities. It should be relatively straightforward for product manufacturers to measure the free velocities at each contact in 1/3 octaves for the sum square value, or by RPM. The source mobilities are average point magnitudes, measured directly (solid lines) or by the two-stage method (red dashed). Alternatively, it may be more convenient to calculate the source mobilities using characteristic plate and beam equations (blue dashed).

Table 4 - Structure-borne sound source data;

Source Type	Measured sum-square free velocity	Average point mobility, measured (solid line), two-stage method (red dashed), calculated (blue dashed)
Compact		
Plate-base		
Cantilever-flange		
Frame		

Also required for the transmitted power, is the receiver mobility, which again is calculated using characteristic plate and beam equations, and a database of building types might be assembled in a similar way as for sources. Here, the building elements are classified as heavyweight: concrete floors and floating floors; masonry walls; or as lightweight: timber-joist floors; timber-frame walls; timber floating floors. Table 5 contains examples of the two basic building element types.

Table 5: Measured and calculated receiver mobility

Receiver type	Receiver mobility
Masonry wall	
Timber joist floor	

Both the magnitude and real part of the receiver mobility are required. However, where the characteristic mobility is sufficient to describe the wall or floor, then real part and magnitude are the same and are frequency invariant. Both source and receiver data could be presented in tabulated form, of course.

8   CONCLUDING REMARKS

This paper has concentrated on advances in measurement and calculation methods for sources of structure-borne sound in buildings. The developments of Standard methods of calculating the sound insulation and impact sound pressure levels of buildings have been included to provide the context of the work on source characterization, i.e. what source quantities are required, and in what form, to provide input data for predicting sound pressure levels when mechanical devices are installed.

Two source quantities are required for estimating the structure-borne power for a wide range of installation conditions: activity (the free velocity or the blocked force of the operating source); source mobility (or the inverse, impedance). The free velocity or blocked force is measured as a sum-square over the contacts of interest. If the source is simultaneously connected to other building elements, then sum-square quantities are measured for these other connections. The free velocity

can be measured directly or by the reception plate method. The source activity is expressed in octaves or third octaves required by practitioners.

The source mobility is obtained as the average of the point mobilities at the contacts. Again, if the source is simultaneously connected to other building elements, then average mobilities are required for these other connections. The source mobility can be measured directly or by the reception plate method and expressed in octaves or third octaves.

Alternatively, the source mobility can be calculated using simple expressions, based on rigid-body behavior, quasi-stationary stiffness, and characteristic values of infinite and semi-infinite plates and beams. Likewise, the receiver mobility of floors and walls can be calculated, based on the characteristic values. Both the real part and the magnitude are required, but where infinite plate/beam behaviour is evident, then the characteristic mobility only is required, which is real-valued.

Using simple classifications of sources and receivers, a data base might be assembled of the quantities required for prediction of the structure-borne power into each building element of interest.

This paper has not been exhaustive in describing recent advances in this area and has been somewhat selective, with some emphasis on the authors' contributions and that of colleagues in Europe. The approaches proposed, for measurement and calculation, require more research and more case studiest and the source and receiver classifications are the authors' and could be expanded.

More work is required on the uncertainties in such simplifying proposals. However, the approaches outlined can be viewed as a framework for meeting practitioners' needs for predicting and assessing structure-borne noise problems in buildings.

ACKNOWLEDGEMENTS

REFERENCES

1. E. Gerretsen, "Calculation of sound transmission between dwellings by partitions and flanking structures", *Applied Acoustics*, **12**, 413-433, (1979).
2. E. Gerretsen, "Calculation of airborne and impact sound insulation between dwellings", *Applied Acoustics*, **19**, 245-264 (1986).
3. *Building acoustics-Estimation of acoustic performance of buildings from the performance of elements, Part 1: Airborne sound insulation between rooms.* International Standard ISO 12354-1, International Organization for Standardization, Geneva, Switzerland (2017).
4. *Building acoustics-Estimation of acoustic performance of buildings from the performance of elements, Part 2: Impact sound insulation between rooms.* International Standard ISO 12354-2, International Organization for Standardization, Geneva, Switzerland (2017).
5. *Acoustics – Laboratory measurement of sound insulation of building elements, Parts 1-5.* International Standard ISO 10140, International Organization for Standardization, Geneva, Switzerland (2010 onwards).
6. *Acoustics – Laboratory and field measurement of flanking transmission of airborne, impact and building service equipment sound between adjoining rooms, Parts 1-4.* International Standard ISO 10848, International Organization for Standardization, Geneva, Switzerland (2017).
7. *Acoustics - Determination of sound power of noise sources.* ISO 3740 (all parts) International Standard ISO 10140, International Organization for Standardization, Geneva, Switzerland (2010 onwards).
8. *Building acoustics-Estimation of acoustic performance of buildings from the performance of elements, Part 5: Sound levels due to the service equipment.* European Standard EN 12354-5, European Committee for Standardization, Brussels, Belgium (2009).
9. *Acoustic properties of building elements and of buildings – Laboratory measurement of structure-borne sound from building services equipment for all installation conditions.* European Standard EN 15657, European Committee for Standardization, Brussels, Belgium (2017).
10. M. Villot, "Predicting in-situ sound levels generated by structure-borne sound sources in buildings", Short Communication, Acta Acustica United with Acustica, Vol.103 (2017) 885-886.
11. F. Schöpfer, C. Hopkins, A. R. Mayr and U. Schanda, "Measurement of Transmission Functions in Lightweight Buildings for the Prediction of Structure-borne Sound Transmission from Machinery", *Acta Acustica united with Acustica* **103**, 451-464, (2017).
12. R.H. Lyon, "Statistical Energy Analysis of Dynamical Systems: Theory and Applications", MIT Press (1975).
13. R.J.M. Craik, "Sound Transmission through Buildings using Statistical Energy Analysis", Gower Publishing Ltd. (1996).
14. C. Hopkins, "Sound Insulation", Elsevier Ltd. (2007).
15. C. Guigou-Carter, M. Villot and R. Wetta, "Prediction method adapted to wood frame lightweight constructions", *Building Acoustics,* **13** (3), 173-188, (2006).
16. M. Villot and C. Guigou-Carter, "Measurement methods adapted to wood frame lightweight constructions", *Building Acoustics,* **13** (3), 189-198, (2006).

17. T. Kihlman, "Urgent need for structure-borne sound source data", *Inter-Noise 78, 343-347,* (1978).

18. T. ten Wolde and G.R. Gadefelt, "Development of standard methods for structure-borne sound emission", *Noise Control Engineering Journal,* **28** (1), 5-14, (1987).

19. E. Gerretsen, "Some practical aspects of the prediction of structure-borne sound caused by house-hold equipment", *Acoustics 08, Paris,* (2008).

20. M. Villot, "Characterization of building equipment", *Applied Acoustics* **61**, 271-283, (2000).

21. B.A.T. Petersson and B.M. Gibbs, "Towards a structure-borne sound source characterization", *Applied Acoustics,* **61** (3), 325-343, (2000).

22. J.M. Mondot and B.A.T. Petersson, "Characterisation of structure-borne sound sources: The source descriptor and the coupling function", *J. Sound Vibr.* **114** (3), 507-518, (1987).

23. A.T. Moorhouse, "On the characteristic power of structure-borne sound sources", *J. Sound Vibr.* **248** (3), 441-459 (2001).

24. B.M. Gibbs, N. Qi and A.T. Moorhouse, "A practical characterization for vibro-acoustic sources in buildings", *Acta Acustica united with Acustica*, **93**, 84-93 (2007).

25. F.A. Firestone, "A new analogy between mechanical and electrical systems", *J. Acoust. Soc. Am.* **4** (3), 249-267, (1933).

26. P. Gardonio and M.M. Brennan, "Mobility and impedance methods in structural dynamics", Chapter 9 in *Advanced Applications in Acoustics, Noise and Vibration*, edited by F.F. Fahy and J. Walker, Spon Press, London (2009).

27. *Acoustics - Characterization of sources of structure-borne sound with respect to sound radiation from connected structures – Measurement of velocity at the contact points of machinery when resiliently mounted.* International Standard ISO 9611, International Organization for Standardization, Geneva, Switzerland (1996).

28. A.T. Moorhouse, A.S. Elliott and T.A. Evans, "In situ measurement of the blocked force of structure-borne sound sources", *J. Sound Vibr.* **325**, 679-685, (2009).

29. R. Breeuwer and J.C. Tucker, "Resilient mounting systems in building", *Applied Acoustics,* **9**, 77-1001, (1976).

30. J. Scheck and B.M. Gibbs, "Impacted lightweight stairs as structure-borne sound sources", *Applied Acoustics*, **90**, 9-20, (2015).

31. L. Cremer, M. Heckl and B.A.T. Petersson, "Structure-borne Sound", 3rd ed., *Springer*, Berlin (2005).

32. K. Larson and C. Simmons, "Measurement of structure-borne sound from building services equipment by a substitution method – Round robin comparisons", *Noise Control Eng. J.* **59**(1), 75-86, (2011).

33. B.M. Gibbs, "Uncertainties in predicting structure-borne sound power input into buildings", *J. Acoustical Soc. Am.* **133** (5), 2678-2689, (2013).

34. P. Hammer and J. Brunskog, "Vibration isolation on lightweight floor structures", *Building Acoustics,* **9** (4), 257-269, (2002).

35. S.H. Yap and B.M. Gibbs, "Structure-borne sound transmission from machines in buildings, part 2: Indirect measurement of force and moment at the machine-receiver interface of a single point connected system by a reciprocal method", *J. Sound and Vibr.* **222** (1), 99-113, (1999).

36. M. Lievens, and M. Vorlander, "Investigation into the Importance of the Degrees of Freedom for the Characterisation of Structure-borne Sound Sources: Case Study of a Washing Machine on a Wooden Floor", *Acta Acustica united with Acustica*, **97**, 940-948 (2011).

37. A.R. Mayr and B.M. Gibbs, "Single equivalent approximation for multiple contact structure-borne sound sources in buildings", *Acta Acustica united with Acustica*, **98**, 402-410, (2012).

38. M.M. Späh and B.M. Gibbs, "Reception plate method for characterization of structure-borne sound sources in buildings: Assumptions and application", *Applied Acoustics* **70**, 361-368 (2009).

39. M.M. Späh and B.M. Gibbs, "Reception plate method for characterization of structure-borne sound sources in buildings: Installed power and sound pressure from laboratory data", *Applied Acoustics* **70**, 1431-1439, (2009).

40. C. Höller and B.M. Gibbs, "Source substitution method for obtaining the power transmission from vibrating sources in buildings", *Applied Acoustics,* **141**, 240-249, (2018).

41. B.M. Gibbs, N. Qi and A. T. Moorhouse, "A practical characterization for vibro-acoustic sources in buildings", *Acta Acustica united with Acustica,* **93**, 84-93, (2007).

42. B.M. Gibbs, R Cookson and N Qi, "Vibration activity and mobility of structure-borne sound sources by a reception plate method", *J. Acoustical Soc. Am.* **123** (6), 4199-4209 (2008).

43. B.M. Gibbs, G. Seiffert and K.H. Lai, "Uncertainties in the Two-Stage Reception Plate Method for Source Characterisation and Prediction of Structure-Borne Sound Power", *Acta Acustica united with Acustica* **102**, 441-451, (2016).

44. A.R. Mayr and B.M. Gibbs, "Approximate method for obtaining source quantities for calculation of structure-borne sound transmission into lightweight buildings", *Applied Acoustics* **110**, 81-90, (2016).

45. K Lai, A T Moorhouse and B M Gibbs, *"*Experimental round-robin evaluation of structure-borne sound source force-power test methods", *Noise Control Engineering Journal* **64** (2), 170-180, (2016).

46. A. Vogel, O. Kornadt, V. Wittstock and W. Scholl, "Assessment of the uncertainties using the "two-stage method" for the characterization of structure-borne sound sources", *Proc. Internoise 2015*, San Francisco.

47. W. Scholl, "Structure-borne sound excitation by occupants in dwellings ("user noise")", *Proc. Novem 2009, Oxford*.

48. V. Wittstock, "Characterisation of structure-borne sound sources in buildings by the two-stage reception plate method", *Proc. Internoise 2010*, Lisbon.

49. Vogel, A., Kornadt, O., Wittstock, V. and Scholl, W., "Application of the two-stage method on the characterization of different structure-borne sound sources and a moment actuator", *Proc. Internoise 2013,* Innsbruck.

50. T.H. Alber, B.M. Gibbs and H-M.Fischer, "Characterisation of valves as sound sources: Structure-borne sound", *Applied Acoustics*, **70**, 661-673, (2009).

51. A. T. Moorhouse and B. M. Gibbs, "Calculation of the mean and maximum mobility for concrete floors"*, Applied Acoustics*, **45**, 227-245, (1995).

52. A.R. Mayr and B.M. Gibbs, "Point and transfer mobility of point-connected ribbed plates", *J. Sound Vib.,* **330**, 4798-4812, (2011).

53. B. M. Gibbs and A. T. Moorhouse, "Case studies of machine bases as structure-borne sound source in buildings", *International Journal of Acoustics and Vibration*, **4** (3), 125-133, (1999).

54. B.A.T. Petersson and J. Plunt, "On effective mobilities in the prediction of structure-borne sound transmission between a source and a receiver structure, Part 2: Estimation of mobilities", *J. Sound Vib.* **82**, 531-540, (1982).